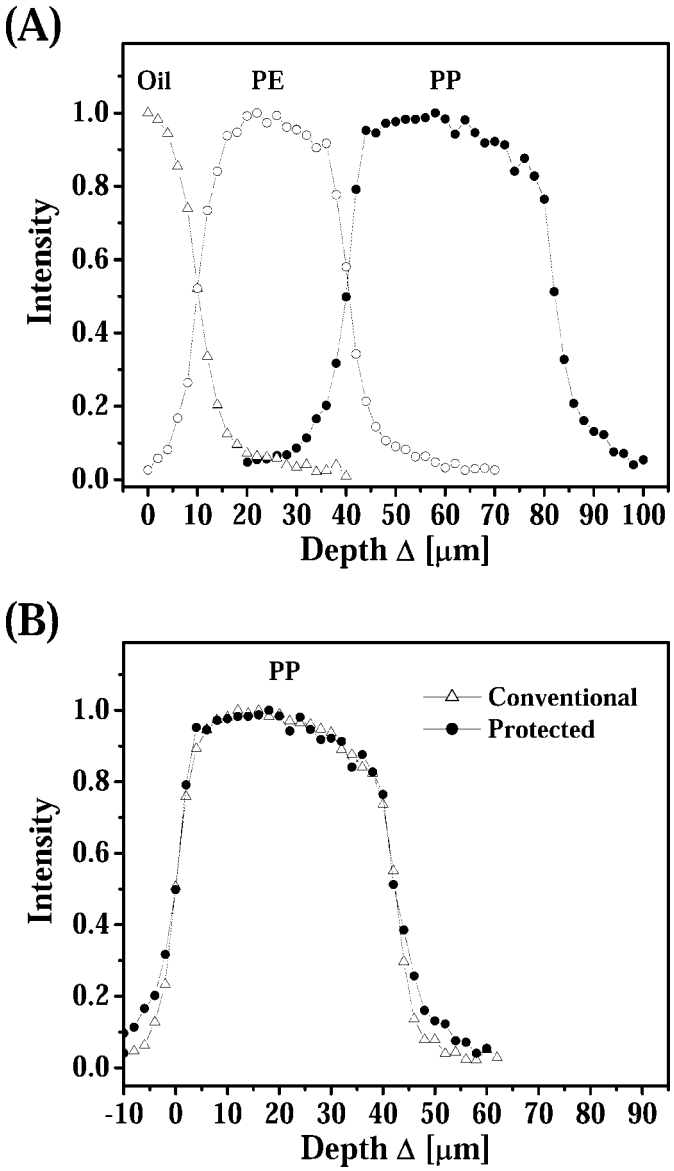


FIG. 2. (**A**) Confocal profiles of the test system; (**B**) Comparison of the confocal response of the PP film, as measured through the protective film and in the conventional way. In all the cases, the objective was an oil immersion Olympus 100× (NA = 1.3), in conjunction with a confocal aperture of 200 μm and a coupling oil with $n = 1.5$.

The FWHM of the corresponding derivative curves is, on average, ~6 μm, somewhat higher that the nominal depth resolution (4.5 μm), but satisfactory for the purposes of the work.

Figure 2B shows a direct comparison between the results obtained with the proposed approach and measurements carried out in the conventional way, i.e., using immersion objectives with the coupling oil directly applied onto the PP film. In the comparison, the PP responses have been shifted with respect to the maximum of the derivative curve of the respective intensity profile and have been scaled with respect to unity. We see that both strategies yielded practically the same confocal response. In terms of collection efficiency of Raman signal, we observed a minor decrease, about 10%, with respect to the conventional approach. Overall, the same good agreement was found for other PP substrates analyzed (films 25 and 65 μm thick).

We conclude that this simple approach efficiently protects the substrate from potential damage by direct contact with the coupling oil, keeping at the same time the benefits of working with immersion optics: almost invariant depth resolution, close to the diffraction limit, and good optical throughput. There are some obvious limitations in terms of specimen dimensions and surface roughness of the sample, but they are not much more stringent that those required for carrying out conventional depth profiling with immersion objectives.

**ACKNOWLEDGMENTS**

This work is part of a project funded by ANPCYT (PICT06-1359) and AECI (A60606).

1. G. J. Puppels, F. F. M. de Mul, C. Otto, J. Greve, M. Robert-Nicoud, D. J. Arndt-Jovin, and T. M. Jovin, Nature (London) **347,** 301 (1990).
2. G. P. Puppels, W. Colier, J. H. F. Olminkhof, C. Otto, F. F. M. de Mul, and J. Greeve, J. Raman Spectrosc. **22,** 217 (1991).
3. N. Everall, Appl. Spectrosc. **54,** 773 (2000).
4. N. Everall, Appl. Spectrosc. **54,** 1515 (2000).
5. N. Everall, Spectroscopy **19,** 22 (2004).
6. N. Everall, Spectroscopy **19,** 16 (2004).
7. K. J. Baldwin and D. N. Batchelder, Appl. Spectrosc. **55,** 517 (2001).
8. C. Sourisseau and P. Maraval, Appl. Spectrosc. **57,** 1324 (2003).
9. N. Everall, J. Lapham, F. Adar, A. Whitley, E. Lee, and S. Mamedov, Appl. Spectrosc. **61,** 251 (2007).
10. J. Vyorykka, J. Halttunen, H. Iitti, J. Tenhunen, T. Vuorinen, and P. Stenius, Appl. Spectrosc. **56,** 776 (2002).
11. F. Adar, C. Naudin, A. Whitley, and R. Bodnar, Appl. Spectrosc. **58,** 1136 (2004).
12. J. P. Tomba, L. M. Arzondo, and J. M. Pastor, Appl. Spectrosc. **61,** 177 (2007).

# A Novel Wavelength Calibration for Fiber-Optical Spectrographs Based on the Grating-Diffractive Equation

**ZHIMIN PENG, QIANSUO YANG,* CHUN LIU, NAIYI ZHU, and ZONGLIN JIANG**

*Laboratory of High Temperature Dynamics, Institute of Mechanics, Chinese Academy of Sciences, 100080 Beijing, China*

Index Headings: **Fiber-optical spectrograph; Wavelength calibration; Standard line spectra; Charge-coupled device; CCD; Low-pressure mercury discharge lamp.**

## INTRODUCTION

Fiber-optical spectrographs can be used for spectral measurement in a spectral area from the ultraviolet–visible to the near-infrared regions because generally the response wave range of the charge-coupled device (CCD) is from 200 to 1100

Received 5 December 2007; accepted 15 April 2008.

* Author to whom correspondence should be sent. E-mail: qsyang@imech.ac.cn.

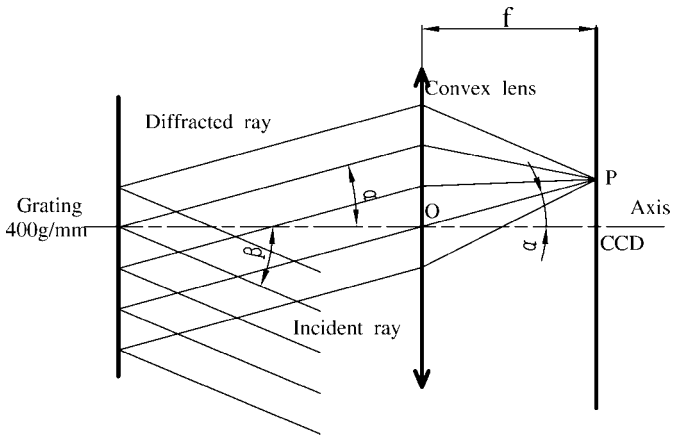


FIG. 1. Equivalent light path of the fiber-optical spectrograph.

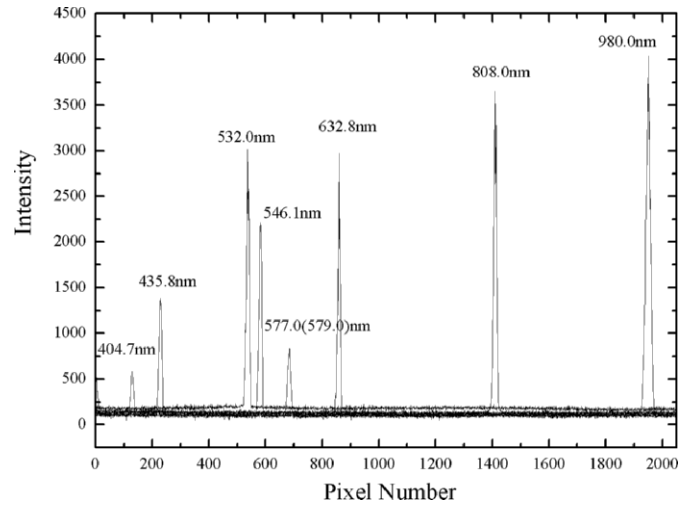


FIG. 2. Spectrum of standard spectral lines.

nm.[1] In application, the wavelength calibration of a fiber-optical spectrograph should be exact before a real spectrum measurement is taken. Thus, determining the corresponding wavelength of the CCD pixel is necessary in a fiber-optical spectrograph.

Several wavelength calibration methods for fiber-optical spectrographs have been introduced in the past. Such methods are based on polynomial expansion, where the precision of the wavelength calibration increases as the expansion series increases. However, the higher the precision of the wavelength, the more the corresponding standard line-spectra are used in the calibration process. In one study, Cho et al. improved the precision of wavelength calibration by introducing sin and cos functions to polynomials.[2] Since then, additional parameters have been introduced into the method, therefore affecting the precision of the wavelength calibration. Moreover, this calibration method comes from polynomial expansion.

In this paper, the researchers introduce a novel wavelength calibration method for fiber-optical spectrographs in which three line spectra with known wavelengths are used in the wavelength calibration process. The method starts from the configuration of the fiber-optical spectrograph and the grating-diffractive equation. The study revealed that the precision of the wavelength calibration is greatly improved over the precision of the previous methods based on polynomial expansion.

## EXPERIMENTAL

Although there are various structures for fiber-optical spectrographs, a typical fiber-optical spectrograph consists of a fiber, a spherical reflector, a grating, a CCD, and a computer system. According to geometrical optical principles, the light path of the fiber-optical spectrograph can be simplified, as shown in Fig. 1. For an actual spectrograph, the first diffractive stripe is used as the detected light. Therefore, the grating-diffractive equation can be written as follows:[3]

$$d(\sin\beta - \sin\alpha) = \lambda \tag{1}$$

where $\lambda$ is the wavelength, $\alpha$ is the diffraction angle for the light with wavelength $\lambda$, $\beta$ is the incident angle, and $d$ is the grating constant.

In the spectrograph used by the researchers in the present study, the CCD was located on the convex lens' focal surface and had 2048 pixels; the dimension of each pixel was about 14 μm. The response wavelength range was 200 nm∼1100 nm. The grating constant $d$ was equal to 2500 nm.

In Fig. 1, if point P corresponds to the $k$th pixel of the CCD, where the ray of wavelength $\lambda$ is focused, one can obtain the following:

$$f\tan\alpha = k\Delta + B \tag{2}$$

where $\Delta$ is the length of each pixel, $f$ is the focal length of the convex lens, and $B$ is a constant. Substituting Eq. 1 into Eq. 2, one can obtain the following equation:

$$\frac{f\left(\sin\beta - \dfrac{\lambda}{d}\right)}{\sqrt{1-\left(\sin\beta - \dfrac{\lambda}{d}\right)^2}} = k\Delta + B \tag{3}$$

By using the definitions $a_1 = B/f$, $a_2 = \Delta/f$, and $a_3 = \sin\beta$, Eq. 3 can be simplified as follows:

$$\frac{\left(a_3 - \dfrac{\lambda}{d}\right)}{\sqrt{1-\left(a_3 - \dfrac{\lambda}{d}\right)^2}} = a_1 + a_2 k \tag{4}$$

Once the assembly of a fiber-optical spectrograph is done, the values of $a_1$, $a_2$, and $a_3$ are fixed. In the experiments pertaining to this paper, low-pressure mercury discharge lamps (404.7 nm, 435.8 nm, 546.1 nm, 577.0 nm, 579.0 nm) and some lasers (532.0 nm, 632.8 nm, 808.0 nm, 980.0 nm) were used as the standard spectral line sources.

The structures of these standard spectral lines were added (see Fig. 2). In the calibration process, the average values of the pixels for each spectral line were obtained by continuous multiple-piece spectra. In the experiment, ten pieces of spectra were obtained continuously. Table I shows the relation of the average values of the pixels to the wavelengths.

Equation 4 shows the three unknown coefficients ($a_1$, $a_2$, and $a_3$). Therefore, the wavelength calibration only requires the data of any three of the standard spectral lines in Table I. After

**TABLE I. The experimental results for the average values of the pixel with the wavelengths.**

| Standard spectral lines ($\lambda$: nm) | 404.7 | 435.8 | 532.0 | 546.1 | 632.8 | 808.0 | 980.0 |
|---|---|---|---|---|---|---|---|
| Number of pixels ($k$) | 128.0 | 229.0 | 538.0 | 583.0 | 858.0 | 1409.0 | 1950.5 |

the three coefficients $a_1$, $a_2$, and $a_3$ are obtained, the researcher can then determine the wavelength value for each pixel based on Eq. 4. Because the process is based on the grating-diffractive equation, the method is named the formula method.

To compare the precision of the wavelength in the formula method with the precision in previous calibration methods, five calibration methods were used; the expression for the relation of the wavelengths to the pixels in these calibration methods can be expressed as follows:[4–7]

Linear method:

$$\lambda = a_1 + a_2 k \tag{5}$$

Quadratic method:

$$\lambda = a_1 + a_2 k + a_3 k^2 \tag{6}$$

Cubic method:

$$\lambda = a_1 + a_2 k + a_3 k^2 + a_4 k^3 \tag{7}$$

Trigonometric method 1:

$$\lambda = a_1 + a_2 k + a_3 \sin\left(\frac{k\pi}{n_\mathrm{p}}\right) \tag{8}$$

Trigonometric method 2:

$$\lambda = a_1 + a_2 k + a_3 \sin\left(\frac{k\pi}{n_\mathrm{p}}\right) + a_4 \cos\left(\frac{k\pi}{n_\mathrm{p}}\right) \tag{9}$$

Formula method:

$$\frac{\left(a_3 - \frac{\lambda}{d}\right)}{\sqrt{1 - \left(a_3 - \frac{\lambda}{d}\right)^2}} = a_1 + a_2 k \tag{10}$$

where $a_i$ in each equation are the unknown coefficients, $n_\mathrm{p}$ is the number of pixels within a given spectral range, and $n_\mathrm{p} = 2048$ in our device.[1]

For the convenience of comparison, standard spectral lines for all methods were chosen as follows:[8]

Linear method: 404.7 nm, 808.0 nm;

Quadratic method, trigonometric method 1, and formula method: 404.7 nm, 632.8 nm, 808.0 nm;

Cubic method and trigonometric method 2: 404.7 nm, 532.0 nm, 632.8 nm, 808.0 nm.

The standard error of the estimate (SEE) was used as a criterion for the goodness of fit, where SEE is given by Eq. 11, $\hat{\lambda}_i$ and $\lambda_i$ are the estimated and actual wavelengths of standard spectral lines, and $n$ and $p$ are the number of standard spectral lines and the number of coefficients in the models, respectively.[1]

$$SEE = \sqrt{\frac{\sum_1^n (\hat{\lambda}_i - \lambda_i)^2}{n - p}} \tag{11}$$

## RESULTS AND DISCUSSION

Based on the analysis given above, it can be inferred that the linear, quadratic, trigonometric, and cubic methods belong to the family of mathematical approximation methods and do not refer to the configuration of the fiber-optical spectrograph; therefore, the methods apply to any fiber-optical spectrograph. The formula method originates directly from the configuration of the fiber-optical spectrograph. The calibration formula is derived from the grating-diffractive equation. While there are many kinds of structures for fiber-optical spectrographs, the configuration of a fiber-optical spectrograph is the same and the method is valid for different types of fiber-optical spectrographs. It is fully known that the corresponding wavelength of each standard spectral line to the CCD pixel requires accurate confirmation in the calibration process.

Table II lists the calibration wavelengths (cal. wavelengths) and calibrated errors (cal. errors) of all the methods; the corresponding error results are shown in Fig. 3. Based on Table II, one can conclude that the calibrated errors of the formula method are smaller than those of any other calibration method.

**TABLE II. The calibrated errors (cal. errors) between the calibration wavelengths (cal. wavelengths) and standard wavelengths of each standard spectral line. SEE is the standard error of estimate.**

| Methods | | Standard spectral lines (nm) 404.7 | 435.8 | 532.0 | 546.1 | 632.8 | 808.0 | 980.0 | SEE |
|---|---|---|---|---|---|---|---|---|---|
| Linear | Cal. wavelengths | 404.67 | 436.47 | 533.75 | 547.91 | 634.50 | 807.97 | 978.45 | |
| | Cal. errors | −0.03 | 0.67 | 1.75 | 1.81 | 1.70 | −0.03 | 1.55 | 1.55 |
| Quadratic | Cal. wavelengths | 404.67 | 435.96 | 532.22 | 546.30 | 632.77 | 807.97 | 982.69 | |
| | Cal. errors | −0.03 | 0.16 | 0.22 | 0.20 | −0.03 | −0.03 | 2.69 | 1.36 |
| Cubic | Cal. wavelengths | 404.67 | 435.79 | 531.97 | 546.08 | 632.77 | 807.97 | 980.35 | |
| | Cal. errors | −0.03 | −0.01 | −0.03 | −0.02 | −0.03 | −0.03 | 0.35 | 0.21 |
| Trigonometric 1 | Cal. wavelengths | 404.67 | 436.05 | 532.33 | 546.41 | 632.77 | 807.97 | 982.44 | |
| | Cal. errors | −0.03 | 0.25 | 0.33 | 0.31 | −0.03 | −0.03 | 2.44 | 1.25 |
| Trigonometric 2 | Cal. wavelengths | 404.67 | 435.82 | 531.97 | 546.07 | 632.77 | 807.97 | 979.48 | |
| | Cal. errors | −0.03 | 0.02 | −0.03 | −0.03 | −0.03 | −0.03 | −0.52 | 0.30 |
| Formula | Cal. wavelengths | 404.67 | 435.77 | 531.94 | 546.05 | 632.76 | 807.96 | 979.95 | |
| | Cal. errors | −0.03 | −0.03 | −0.06 | −0.05 | −0.04 | −0.04 | −0.05 | 0.05 |

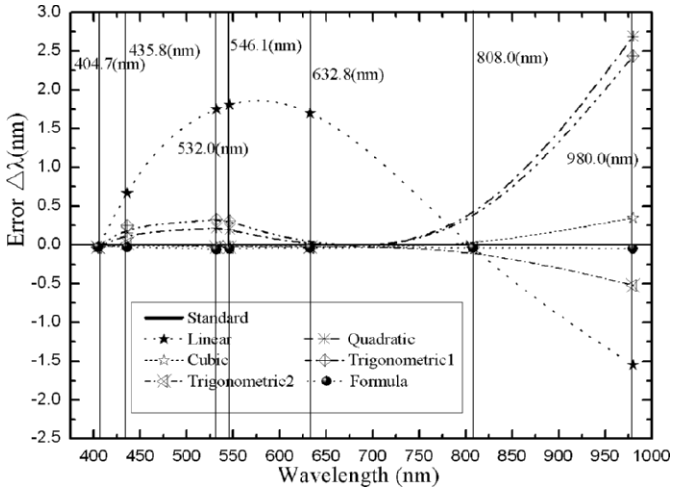


FIG. 3. The corresponding calibrated errors for different wavelengths for all calibration methods.

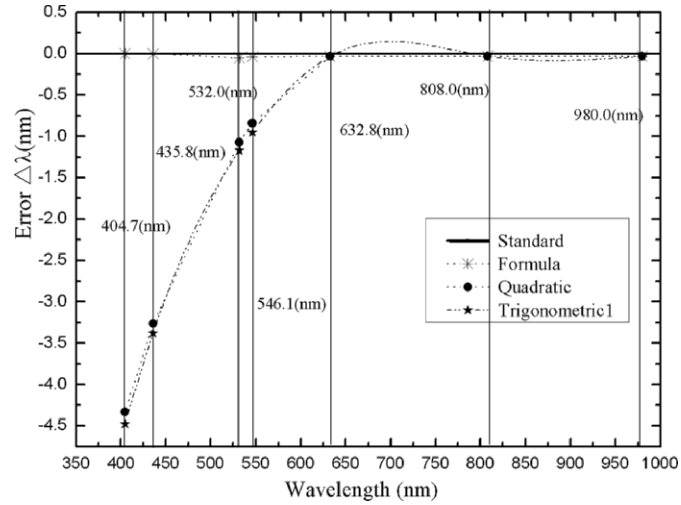


FIG. 4. Calibrated wavelengths and corresponding errors for the formula, quadratic, and trigonometric 1 methods.

To understand each method, it is important to be familiar with the characteristics of all the methods.

The linear method was the simplest, but the corresponding calibrated error was the biggest. The quadratic method was applied broadly in wavelength calibration for the fiber-optical spectrograph, and the corresponding calibrated error was also big. Compared with the quadratic method, a high-order term was introduced in the cubic method, and therefore the calibrated errors were effectively reduced. However, four standard spectral lines were required in the calibration.

The sin function was introduced in trigonometric method 1. Because there were only odd terms to expand the sin function, the calibration precision was less improved than for the quadratic method. Moreover, in the formula of trigonometric method 1, the calibrated errors were also a function of $n_p$, where it was not easy to assign a value to it for the smallest of all the wavelength errors. Sin and cos were introduced in trigonometric method 2, and the calibrated errors were reduced effectively. However, four standard spectral lines were required for the calibration. Meanwhile, a similar question occurred where it was also necessary for $n_p$ to be set to an appropriate value because the wavelength precision was also related to the value of $n_p$, as it was for trigonometric method 1.

For all the calibration methods above, the standard spectral lines used for calibration had strict demands: their spans must be comparatively large and uniformly distributed.

In conclusion, the calibrated errors of the linear, quadratic, trigonometric, and cubic methods resulted from the lack of high-order items because of mathematical approximation. The high-order items were neglected in the linear, quadratic, and cubic methods. Therefore, the precision of wavelength calibration is improved in theory with the increase of high-order items. The standard line spectra used for calibration also increased. Although sin and cos were introduced in the trigonometric methods 1 and 2, and the high-order items for the expansion of the function were infinite, it was not easy to set a suitable value for $n_p$ with the smallest error, which affected the coefficient of the high-order items.

The formula method originated directly from the configuration of the fiber-optical spectrograph; the calibration formula was based on the grating-diffractive equation. The only parameter related to the configuration of the spectrograph was the grating constant, $d$. Compared with the others methods, the formula method had some natural advantages. Through this paper, the precision of wavelength calibration was improved greatly where only three standard spectral lines were used. Its calibrated errors can be controlled within 0.05 nm and are small not only in the range of standard spectral lines but also in the range compared with the above-discussed methods.

To illustrate the advantages of the formula method, a comparison of the experimental results from the formula method, the quadratic method, and trigonometric method 1 is shown in Table III and Fig. 4, where the three standard spectral lines of 632.8 nm, 808.0 nm, and 980.0 nm are used in the calibration process because they are not uniformly distributed. Based on Fig. 4, one can see that the span and the distribution

**TABLE III. The calibrated errors (cal. errors) between the calibration wavelengths (cal. wavelengths) and standard wavelengths of each standard spectral line. SEE is the standard error of estimate.**

| Methods | | Standard spectral lines (nm) | | | | | | | |
|---|---|---|---|---|---|---|---|---|---|
| | | 404.7 | 435.8 | 532.0 | 546.1 | 632.8 | 808.0 | 980.0 | SEE |
| Quadratic | Cal. wavelengths | 400.37 | 432.54 | 530.93 | 545.26 | 632.77 | 807.97 | 979.97 | |
| | Cal. errors | −4.33 | −3.26 | −1.07 | −0.84 | −0.03 | −0.03 | −0.03 | 2.79 |
| Trigonometric 1 | Cal. wavelengths | 400.34 | 432.51 | 530.92 | 545.24 | 632.77 | 807.97 | 979.97 | |
| | Cal. errors | −4.36 | −3.29 | −1.08 | −0.86 | −0.03 | −0.03 | −0.03 | 2.82 |
| Formula | Cal. wavelengths | 404.70 | 435.8 | 531.95 | 546.06 | 632.77 | 807.97 | 979.97 | |
| | Cal. errors | 0.00 | 0.00 | −0.05 | −0.04 | −0.03 | −0.03 | −0.03 | 0.04 |

of standard spectral lines have almost no effect on the calibration results for the formula method, with the biggest error at only 0.05 nm. For the quadratic or trigonometric method 1, however, the wavelength errors depend strongly on the span and the distribution of the standard spectral lines.

The reason that there were small errors in the formula method is that there were infinite high-order items after the formula expression was expanded. In the experiment, when the first three items of the formula expression were used, the precision of the wavelength increased almost an order with respect to the quadratic method; the corresponding calibration results approximately reached the precision of the formula method, although its expression form was the same as that of the quadratic method. In fact, there were some factors for the calibration error in the formula method such as chromatic aberration, spherical aberration, and diffraction effects. However, these factors had little effect on the calibration results.

## CONCLUSION

In summary, the linear, quadratic, trigonometric, and cubic methods are all based on polynomial expansion. The calibrated errors result from high-order items, and the precision of the wavelength calibration is gradually improved in theory with the increase of the expansion series. The formula method originates directly from the configuration of the spectrograph and is based on the grating-diffractive equation. Therefore, the wavelength precision in the formula method is much higher than the precision in previous methods.

**ACKNOWLEDGMENTS**

We acknowledge the financial support from the National Science Foundation of China under Grant No.10472123 and the Innovation Project of Chinese Academy of Sciences.

1. Z. Bo and W. Zhiyu, Semicond. Optoelectron. **28,** 147 (2007).
2. J. H. Cho, P. J. Gemperline, and D. Walker, Appl. Spectrosc. **47,** 1841 (1995).
3. F. Zhiqing, B. Lan, and L. Futian, Guangxue Xuebao/Acta Opt. Sin. **24(3),** 393 (2004).
4. American Society for Testing and Materials, "Standard Method for Describing and Measuring Performance of Ultraviolet, Visible, and Near Infrared Spectrophotometers", in *Annual Book of ASTM Standards, 14.01, E275* (ASTM, Gaithersburg, MD, 1987).
5. C. H. Tseng, J. F. Ford, C. K. Mann, and T. J. Vickers, Appl. Spectrosc. **47,** 1808 (1993).
6. J. T. Brownrigg, Appl. Spectrosc. **47,** 1007 (1993).
7. G. Polder and G. W. A. M. van der Heijden, Proc. SPIE-Int. Soc. Opt. Eng. **4548,** 10 (2001).
8. L. Shurong, et al., New Technol. New Proc. **10,** 14 (2002).